

0) The section 1 and section 2 will be combined into one section of introduction and be shortened to less than 900 words.

1) Explanation of the used methods

(1) LPJ setting up

Surfaces of monthly mean air temperature, monthly mean precipitation, monthly wet days and monthly percentage of full sunshine were generated by using HASM to interpolating observations from 752 weather station scattered over China. In addition to the interpolated surfaces on spatial resolution of $5\text{km} \times 5\text{km}$, inputs of local information in China include annual atmospheric CO_2 concentration, soil texture class and the plant functional types.

(2) HASM-SOA

In terms of the fundamental theorem of surfaces, a surface is uniquely defined by the first fundamental coefficients and the second fundamental coefficients. The first fundamental coefficients are used to express the intrinsic geometric properties that do not depend on the shape of the surface, but only on measurements that we can carry out while on the surface itself. The second fundamental coefficients reflect the local warping of the surface, which can be observed from outside the surface (Yue et al. 2016).

If $\{(x_i, y_j)\}$ is an orthogonal division of a computational domain and h represents simulation step length, the central point of lattice (x_i, y_j) could be expressed as

$(0.5h + (i-1)h, 0.5h + (j-1)h)$, in which $i = 0, 1, 2, \dots, I, I+1$ and $j = 0, 1, 2, \dots, J, J+1$. If $f_{ij}^{(n)}$ ($n \geq 0$) represents the iterants of $f(x, y)$ at (x_i, y_j) in the n th iterative step, in which $\{f_{i,j}^{(0)}\}$ are results from SOA, the iterative formulation of master equation set of the method for high accuracy surface modeling (HASM) can be formulated as (Yue et al. 2013b; Zhao and Yue 2014 a, b),

$$\begin{aligned} & \frac{-f_{i+2,j}^{(n+1)} + 16f_{i+1,j}^{(n+1)} - 30f_{i,j}^{(n+1)} + 16f_{i-1,j}^{(n+1)} - f_{i-2,j}^{(n+1)}}{12h^2} \\ &= (\Gamma_{11}^1)^{(n)}_{i,j} \frac{f_{i+1,j}^{(n)} - f_{i-1,j}^{(n)}}{2h} + (\Gamma_{11}^2)^{(n)}_{i,j} \frac{f_{i,j+1}^{(n)} - f_{i,j-1}^{(n)}}{2h} + \frac{L_{ij}^{(n)}}{\sqrt{E_{i,j}^{(n)} + G_{i,j}^{(n)} - 1}} \end{aligned} \quad (1)$$

$$\begin{aligned} & \frac{-f_{i,j+2}^{(n+1)} + 16f_{i,j+1}^{(n+1)} - 30f_{i,j}^{(n+1)} + 16f_{i,j-1}^{(n+1)} - f_{i,j-2}^{(n+1)}}{12h^2} \\ &= (\Gamma_{22}^1)^{(n)}_{i,j} \frac{f_{i+1,j}^{(n)} - f_{i-1,j}^{(n)}}{2h} + (\Gamma_{22}^2)^{(n)}_{i,j} \frac{f_{i,j+1}^{(n)} - f_{i,j-1}^{(n)}}{2h} + \frac{N_{ij}^{(n)}}{\sqrt{E_{i,j}^{(n)} + G_{i,j}^{(n)} - 1}} \end{aligned} \quad (2)$$

$$\begin{aligned} & \frac{f_{i+1,j+1}^{(n+1)} - f_{i+1,j}^{(n+1)} - f_{i,j+1}^{(n+1)} + 2f_{i,j}^{(n+1)} + f_{i-1,j}^{(n+1)} - f_{i,j-1}^{(n+1)} + f_{i-1,j-1}^{(n+1)}}{2h^2} \\ &= (\Gamma_{12}^1)^{(n)}_{i,j} \frac{f_{i+1,j}^{(n)} - f_{i-1,j}^{(n)}}{2h} + (\Gamma_{12}^2)^{(n)}_{i,j} \frac{f_{i,j+1}^{(n)} - f_{i,j-1}^{(n)}}{2h} + \frac{M_{ij}^{(n)}}{\sqrt{E_{i,j}^{(n)} + G_{i,j}^{(n)} - 1}} \end{aligned} \quad (3)$$

where $E_{ij}^{(n)}$, $F_{ij}^{(n)}$ and $G_{ij}^{(n)}$ are the iterants of the first fundamental coefficients at the n th iterative step; $L_{ij}^{(n)}$, $M_{ij}^{(n)}$ and $N_{ij}^{(n)}$ represent the iterants of the second fundamental coefficients at the n th iterative step; $(\Gamma_{11}^1)^{(n)}$, $(\Gamma_{11}^2)^{(n)}$, $(\Gamma_{22}^1)^{(n)}$ and $(\Gamma_{22}^2)^{(n)}$ the iterants of the Christoffel symbols of the second kind at the n th iterative step, which depend only upon the first fundamental coefficients and their derivatives.

The matrix formulation of HASM master equations can be respectively expressed as,

$$\mathbf{A} \cdot \mathbf{z}^{(n+1)} = \mathbf{d}^{(n)} \quad (4)$$

$$\mathbf{B} \cdot \mathbf{z}^{(n+1)} = \mathbf{q}^{(n)} \quad (5)$$

$$\mathbf{C} \cdot \mathbf{z}^{(n+1)} = \mathbf{p}^{(n)} \quad (6)$$

where \mathbf{A} , \mathbf{B} and \mathbf{C} represent coefficient matrixes of the first equation, the second equation and the third equation; $\mathbf{d}^{(n)}$, $\mathbf{q}^{(n)}$ and $\mathbf{p}^{(n)}$ are right-hand side vectors of the three equations respectively;

$$\mathbf{z}^{(n+1)} = \left(f_{1,1}^{(n+1)}, \dots, f_{1,J}^{(n+1)}, \dots, f_{I,1}^{(n+1)}, \dots, f_{I,J}^{(n+1)} \right)^T = \left(z_1^{(n+1)}, \dots, z_J^{(n+1)}, \dots, z_{(I-1)J+1}^{(n+1)}, \dots, z_{IJ}^{(n+1)} \right)^T,$$

$f_{i,j}^{(n)}$ is the value of the n th iteration of $f(x, y)$ at grid cell (x_i, y_j) ; $z_{(i-1)J+j}^{(n+1)} = f_{i,j}^{(n+1)}$

for $1 \leq i \leq I$, $1 \leq j \leq J$.

If $\bar{f}_{i,j}$ is BCS at the p th sample plot (x_i, y_j) , $s_{p,(i-1)J+j} = 1$, $k_p = \bar{f}_{i,j}$. There is only one non-zero element, 1, in every row of the coefficient matrix, \mathbf{S} , making it a sparse matrix. The solution procedure of HASM, taking the BCS at the sampled plots as its optimum control constraints and results from SOA as its driving field, can be transformed into solving the following linear equation set in terms of least squares principle

$$\begin{bmatrix} \mathbf{A}^T & \mathbf{B}^T & \mathbf{C}^T & \lambda \cdot \mathbf{S}^T \end{bmatrix} \begin{bmatrix} \mathbf{A} \\ \mathbf{B} \\ \mathbf{C} \\ \lambda \cdot \mathbf{S} \end{bmatrix} \mathbf{z}^{(n+1)} = \begin{bmatrix} \mathbf{A}^T & \mathbf{B}^T & \mathbf{C}^T & \lambda \cdot \mathbf{S}^T \end{bmatrix} \begin{bmatrix} \mathbf{d}^{(n)} \\ \mathbf{q}^{(n)} \\ \mathbf{p}^{(n)} \\ \lambda \cdot \mathbf{k} \end{bmatrix} \quad (7)$$

The parameter λ is the weight of the sample plots and determines the contribution of the sample plots to the simulated surface. λ could be a real number, which means all sample plots have the same weight, or a sector, which means every sample plot has its own weight. An area affected by a sample plot in a heterogeneous region is smaller than in a homogeneous region. Therefore, a smaller value of λ is

selected in a heterogeneous region and a bigger value of λ is selected in a homogeneous region.

2) Scatter diagrams and comparison with other results

(1) Scatter diagrams

The scatter diagrams of simulated BCD against observed BCD indicate that the BCD surface created by Kriging interpolation exhibit a higher correlation with observed BCD, $R^2=0.826$. But Kriging interpolation has a big error in the regions, Xizang/Tibet and Xinjing, where the biggest BCD happened. BCD was overestimated in Xizang and underestimated in Xinjiang (Figure C2a). BCD surface created by SOA has a good correlation coefficient, $R^2= 0.627$, with the observed one. The SOA results show that BCDs in higher and lower latitudes are bigger than the ones in middle latitudes, except the ones in Xinjiang and Xizang. BCD was overestimated in Xinjiang but underestimated in Xizang (Figure C2b). LPJ overestimated BCDs in almost all regions except that it underestimated the ones in Xizang, Xinjiang and Shanxi provinces (Figure C2c). Surface of BCDs generated by HASM-SOA has the best correlation with the observed one, $R^2=0.943$. Especially, it has the smallest errors in the regions of Xizang and Xinjiang, comparing with other methods (Figure C2d).

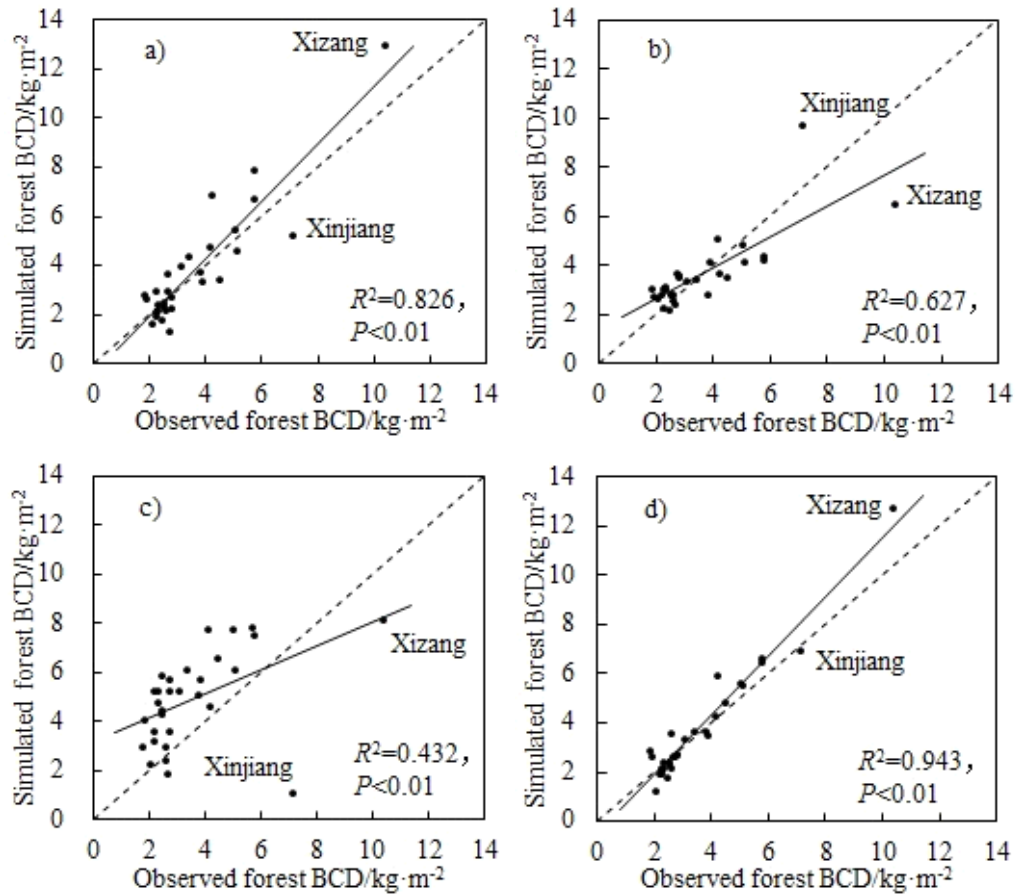


Figure C2. The scatter diagrams of simulated BCD against observed BCD: a) Kriging, b) SOA, c) LPJ-DGVM, and d) HASM-SOA

(2) Comparison with other results

The results from HASM-SOA are different more or less from other studies. For instances, annual growth of total BCS, from period 1 (circa 1986) to period 5 (circa 2006) in China was 0.112 PgCyr^{-1} according to our estimation. It was higher than estimation from Zhang *et al.* (2013), which was 0.103 PgCyr^{-1} . However, from period 3 (circa 1996) to period 5 (circa 2006), our estimation, 0.148 PgCyr^{-1} , was lower than 0.174 PgCyr^{-1} , estimated by Zhang *et al.* (2013). From period 4 (circa 2001) to period 5 (circa 2006), 0.14 PgCyr^{-1} estimated by HASM-SOA was twice as big as the

one done by Liu Y Y *et al.* (2015).

References

Fang J Y, Chen A P, Peng C H, et al. 2001. Changes in forest biomass carbon storage in China between 1949 and 1998. *Science*, 292 (5525): 2320-2322

Zhang C H, Ju W M, Chen J M, Zan M Li D Q, Zhou Y L and Wang X Q. 2013. China's forest biomass carbon sink based on seven inventories from 1973 to 2008. *Climatic Change*, 118: 933–948

Liu Y Y, van Dijk A I J M, de Jeu R A M, *et al.* 2015. Recent reversal in loss of global terrestrial biomass. *Nature climate change*, DOI: 10.1038/NCLIMATE2581

3) The section 1 and section 2 will be combined into one section of introduction and be shortened to less than 900 words.

4) The title is to be changed to “Analyzing the uncertainty of estimating forest carbon stocks in China”

5) We agree.

6) Table 2 and table 3 are to be deleted.

The data of Table 1 are from the following references:

- Office of Converting Farmland to Forestry, State Forestry Administration of China: A new round of the overall concept of returning farmland to forest and grass, Newsletter for Converting Farmland to Forestry, 194, 1-2, 2014 (in Chinese).
- Office of Converting Farmland to Forestry, State Forestry Administration of China: New Year's Speech, Newsletter for Converting Farmland to Forestry, 198, 1-2, 2016 (in Chinese).

7) The forest distribution data were created by combining Vegetation Map of the People's Republic of China (Editorial Committee of Vegetation Map of China, 2007) with a vegetation map from forest inventory conducted during the period from 2004 to 2008 (State Forestry Administration of China, 2009). The former has a detail classification of plant functional types and matches phenological and regional characters of forests in China, but it is not so exact. The latter exhibits the truth of forest distribution in the period of the forest inventory, but its classification has much less plant functional types. The combination of the two kinds of maps keeps their own advantages.

References

Editorial Committee of Vegetation Map of China, 2007. Vegetation Map of the People's Republic of China. Geological Publishing House, Beijing (in Chinese).

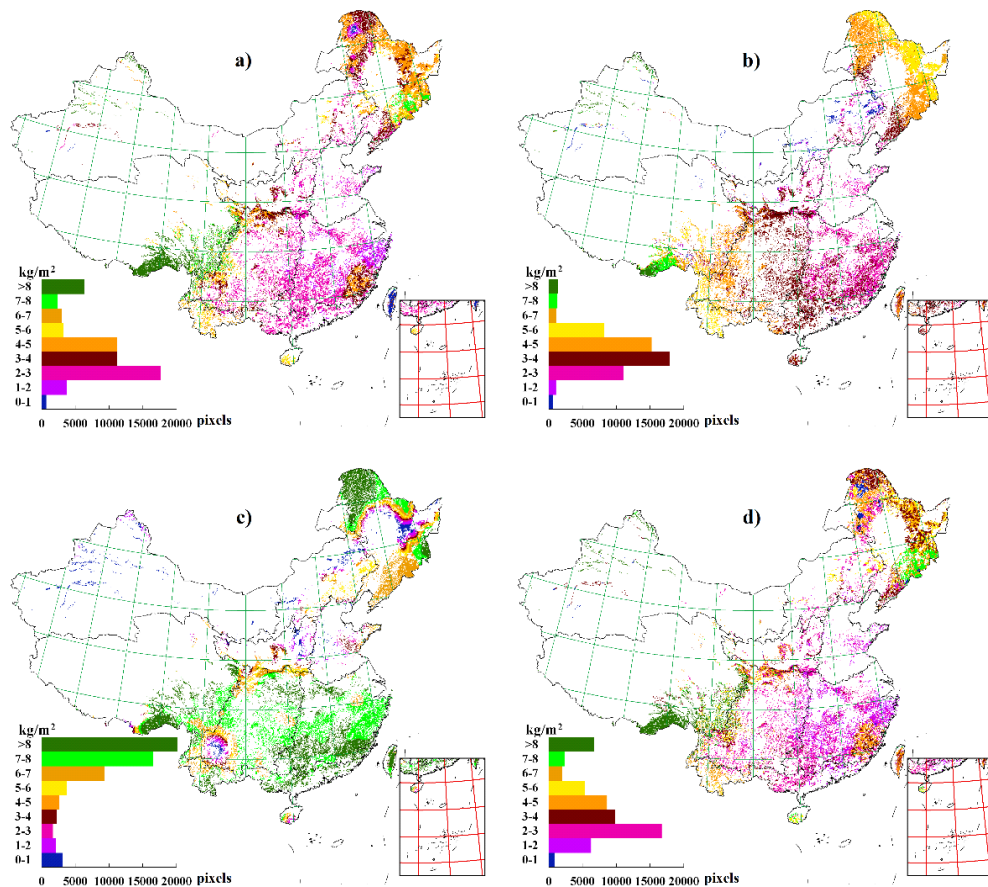
State Forestry Administration of China, 2009. National Forest Report (2004-2008).

China Forestry Publishing House, Beijing (in Chinese).

8) BEF is the abbreviation of biomass expansion factor (see 19544, line 1).

9) The biomass carbon stock and biomass carbon density are respectively abbreviated to BCS and BCD instead of CS/MACS/AMCS and CD/MACD/AMCD.

10) Figure 2 is to be improved as follows by adding histograms of carbon values for the different methods as a first rough comparison.



The spatial distribution of forest biomass BCDs estimated during the period 2004-2008 in China by using:

a) Kriging; b) SOA; c) LPJ and d) HASM-SOA

11) Results related to HASM-LPJ have been deleted. We might also like to delete the results from LPJ because we might not use LPJ correctly in this paper.

12) “mean annual carbon stocks” is a mistake. It means BCS.

13) We agree.

14) The biomass carbon stock and biomass carbon density are respectively abbreviated to BCS and BCD instead of CS/MACS/AMCS and CD/MACD/AMCD.

15) The Table 1 has no change. Table 2 and table 3 are deleted. Table 4 and table 5 are combined and the new table is labelled as Table 2. The original Table 6 renumbered as Table 3. The original Table 7 is renumbered as table 4; The original Table 8 and table 9 are combined and the new table is numbered as Table 5. The Table 2 and Table 5 are modified as follows:

Table 2. Biomass carbon stocks and biomass carbon densities as well as their errors produced by different methods.

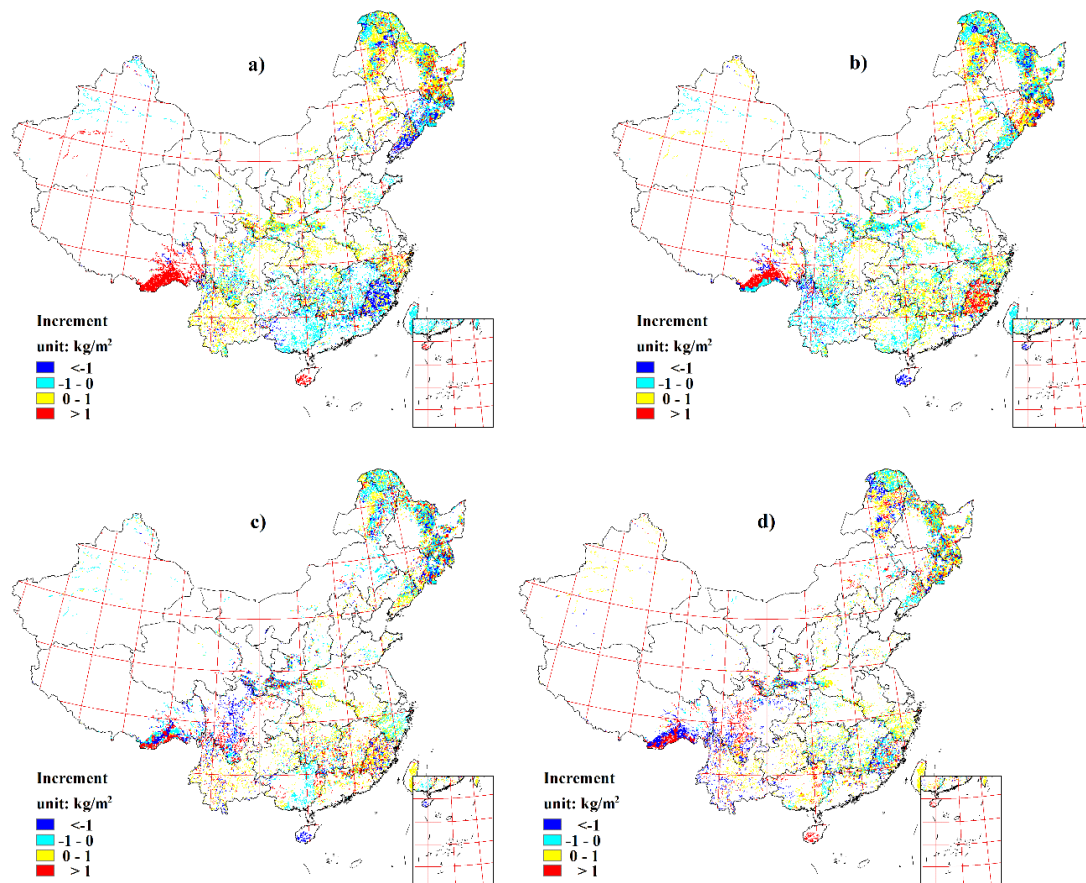
Method	Calculated object	Coniferous forests	Mixed forests	Broadleaf forests	Total	MAE (kg m ⁻²)	MRE (%)
LPJ	BCS (Pg)	3.82	0.57	6.14	10.53	3.12	79.33

	BCD (kg m ⁻²)	6.06	6.18	7.38			
SOA	BCS (Pg)	2.48	0.46	3.61	6.55	1.92	48.77
	BCD (kg m ⁻²)	3.94	4.93	4.34			
Kriging	BCS (Pg)	2.76	0.39	4.11	7.26	1.97	50.12
	BCD (kg m ⁻²)	4.38	4.24	4.94			
HASM-SOA	BCS (Pg)	2.74	0.39	3.95	7.08	0.89	22.71
	BCD (kg m ⁻²)	4.35	4.2	4.74			

Table 5 Biomass carbon stocks and biomass carbon densities estimated by HASM-SOA

Regions	Calculation object	Period 1	Period 2	Period 3	Period 4	Period 5
R1	BCS (Pg)	0.16	0.17	0.17	0.2	0.28
	BCD (kg m ⁻²)	2.67	2.71	2.88	2.98	3.71
R2	BCS (Pg)	0.15	0.16	0.15	0.18	0.2
	BCD (kg m ⁻²)	6.36	6.27	6.25	6.23	6.33
R3	BCS (Pg)	1.59	1.64	1.64	1.77	2.01
	BCD (kg m ⁻²)	4.49	4.42	4.5	4.43	4.44
R4	BCS (Pg)	0.13	0.15	0.14	0.16	0.19
	BCD (kg m ⁻²)	3.04	3.23	3.13	3.15	3.27
R5	BCS (Pg)	0.99	1.57	1.64	1.94	2.03
	BCD (kg m ⁻²)	6.72	10.15	10.83	11.49	10.53
R6	BCS (Pg)	0.82	0.87	0.82	0.96	1.03
	BCD (kg m ⁻²)	3.73	3.78	3.66	3.88	3.67
R7	BCS (Pg)	0.36	0.39	0.37	0.4	0.42
	BCD (kg m ⁻²)	3.64	3.79	3.66	3.54	3.69
R8	BCS (Pg)	0.03	0.04	0.04	0.05	0.06
	BCD (kg m ⁻²)	1.52	1.64	1.89	1.89	2.14
R9	BCS (Pg)	0.62	0.56	0.62	0.73	0.87
	BCD (kg m ⁻²)	2.36	2.05	2.3	2.51	2.6
The whole of China	BCS (Pg)	4.84	5.55	5.6	6.38	7.08
	BCD (kg m ⁻²)	4	4.32	4.33	4.47	4.55
	Area (million km ²)	1.2101	1.2864	1.292	1.4279	1.5559

16) The increment map of biomass carbon stocks from comparing two adjacent periods



a) BCS in Period 2 minus BCS in Period 1, b) BCS in Period 3 minus BCS in Period 2, c) BCS in Period 4 minus BCS in Period 3, and d) BCS in Period 5 minus BCS in Period 4